Artificial Hawking Radiation in Non-Hermitian Parity-Time Symmetric Systems

Marcus Stålhammar[1], Jorge Larana-Aragon[1], Lukas Rødland[1], and Flore K. Kunst[2]
[1]*Department of Physics, Stockholm University, AlbaNova University Center, 106 91 Stockholm, Sweden and*
[2]*Max-Planck-Institut für Quantenoptik, Hans-Kopfermann-Straße 1, 85748 Garching, Germany*

We show that the exceptional surfaces of linear three-dimensional non-Hermitian parity-time-symmetric two-band models attain the form of topologically stable tilted exceptional cones. By relating the exceptional cones to energy cones of two-dimensional Hermitian parity-time-symmetric two-band models, we find a connection between the exceptional cone and the light cone of an observer in the vicinity of a Schwarzschild black hole. When the cone overtilts, light-like particle-antiparticle pairs are created resembling Hawking radiation. We also investigate dissipative features of the non-Hermitian Hamiltonian related to the latter and comment on potential realizations in laboratory setups.

I. INTRODUCTION

Since the experimental discovery of the quantum Hall effect in the 1980s [1], topology has played a prominent role in condensed matter physics. A large part of the studies during the last decades have been devoted to gapped topological insulators [2, 3] and gapless semimetals, such as graphene [4] and Weyl semimetals (WSMs) [5], whose Bloch bands are characterized by distinct topological invariants [6]. The progress in the latter led to the realization of the elusive Weyl fermions which, despite evading discovery for nearly a century after being theoretically predicted [7], were realized as quasi-particles near band crossings in WSMs [8–10]. Generically, such band crossings occur in three dimensions (3D), but in the presence of discrete symmetries, e.g., parity-time ($\mathcal{PT}$) symmetry, topologically stable symmetry-protected nodal points can occur in 2D [11]. As a consequence, the nodal points in 3D are enhanced to knotted nodal lines [12–17]. Furthermore, the cone-like dispersion close to nodal points, both in 2D and 3D, has suggested a possible relation to spacetime light cones [18]. In particular, recent works [16, 19–22] have proposed a relation between the transition from type I to type II WSMs (as the Weyl cone overtilts) and the tilting of an observer's light cone when crossing the black hole horizon (in the infalling coordinate frame).

Recently, many studies of topological phases have focused on non-Hermitian (NH) Hamiltonians, which serve as an effective description of systems subject to gain and loss [23]. Naturally, these Hamiltonians are fundamentally different from their Hermitian counterparts, the most prominent distinction being complex eigenvalues and separate sets of left and right eigenvectors. Furthermore, the nodal structures of NH systems consist of exceptional points (EPs) at which not only the eigenvalues, but also the eigenvectors coalesce [24]. EPs are already topologically stable in 2D [25], and thus 3D systems host knotted lines of EPs [26–32]. As for Hermitian systems, the inclusion of symmetries, such as $\mathcal{PT}$ symmetry, generally enhances the dimension of the exceptional nodal structures, making EPs generic already in 1D [33]. In fact, $\mathcal{PT}$ symmetry has been suggested to replace the Hermiticity constraint in quantum mechanics, motivated by the fact that such systems include a region where the eigenvalues are purely real, called the $\mathcal{PT}$-unbroken phase, while the $\mathcal{PT}$-broken phase results in complex eigenvalues [34]. These two phases are separated by EPs, at which the $\mathcal{PT}$ symmetry is spontaneously broken.

In the spirit of this, we here set out to study the topology of the exceptional nodal structures of NH $\mathcal{PT}$-symmetric systems in 3D. We show that any linear model of this type hosts cones of EPs, which we call exceptional cones (ECs). By relating the model parameters to a $\mathcal{PT}$ symmetry-protected energy cone of a 2D Hermitian Hamiltonian, we prove that the ECs are topologically stable. We furthermore relate the EC to an artificial light cone, and interpret the dissipative behavior on the EC, where $\mathcal{PT}$ symmetry is spontaneously broken, as the creation and emission of light-like particle-antiparticle pairs. Intuitively, this spontaneous radiation of particles resembles spontaneous Hawking radiation in stationary Schwarzschild black holes in 4D-spacetimes. We formalize this intuition at the level of equations. Lastly, we discuss potential realizations in certain laboratory setups and comment on open questions and future research directions.

Throughout this article, we are working in units where $\hbar = c = e = k_{\mathrm{B}} = G_{\mathrm{N}} = 1$.

II. NODAL TOPOLOGY IN TWO-BAND MODELS

In this section, we start with a brief discussion on the topology of nodal structures in general, covering both the Hermitian and the NH cases. We also illustrate how the inclusion of $\mathcal{PT}$ symmetry increases the dimension of the band intersections in both regimes. Then, we specifically study 3D NH models subject to $\mathcal{PT}$ symmetry, and show that the EPs generically constitute a symmetry-protected cone.

A. Dimension of Nodal Structures

A non-interacting Hermitian two-band model in its most general form is given by the following Bloch Hamiltonian in reciprocal space

$$H(\mathbf{k}) = d_0(\mathbf{k})\sigma^0 + \mathbf{d}(\mathbf{k}) \cdot \boldsymbol{\sigma}, \tag{1}$$

where $\mathbf{k}$ is the lattice momentum in the appropriate dimension, σ^0 is the 2×2 identity matrix, $\boldsymbol{\sigma} = (\sigma^x, \sigma^y, \sigma^z)$ are the Pauli matrices, $\mathbf{d}(\mathbf{k}) = [d_x(\mathbf{k}), d_y(\mathbf{k}), d_z(\mathbf{k})]$, and d_μ, $\mu = 0, x, y, z$ are continuously differentiable real-valued

functions of $\mathbf{k}$. From here, we use the notation $d_\mu(\mathbf{k}) =: d_\mu$ for simplicity, restoring the $\mathbf{k}$-dependence when appropriate. We furthermore restrict ourselves to 2D and 3D systems. The corresponding energy eigenvalues are

$$E_\pm = d_0 \pm \sqrt{d_x^2 + d_y^2 + d_z^2}, \tag{2}$$

and the nodal points are given by the intersections of the eigenvalues, which arise from solutions to

$$\sqrt{d_x^2 + d_y^2 + d_z^2} = 0. \tag{3}$$

Nodal points are generically of codimension 3, meaning that they occur in $D = 3$ or higher. There are, however, several ways of reducing the codimension of the nodal structures. The most obvious is if the system of equations in Eq. (3) is underdetermined, but such a case is often not stable and thus relies on fine-tuning. Another option is to impose a symmetry on the system. For the sake of illustration, we consider the effects of $\mathcal{PT}$ symmetry on the nodal structure. We use the following representation,

$$\mathcal{P} = \sigma^z, \quad \mathcal{T} = \sigma^y, \tag{4}$$

such that

$$\mathcal{PT} = -i\sigma^x. \tag{5}$$

Imposing $\mathcal{PT}$ symmetry on a generic two-band Hamiltonian, i.e., in Eq. (1),

$$H_{\mathcal{PT}} = \mathcal{PT} H^*_{\mathcal{PT}} (\mathcal{PT})^{-1}, \tag{6}$$

implies that $d_0, d_x, d_y \in \mathbb{R}$ and $d_z = 0$. Since $d_z = 0$ is satisfied for all $\mathbf{k}$ as a consequence of the symmetry, the nodal structure is determined by a system of merely two equations. Therefore, $\mathcal{PT}$-symmetric 2D systems generically host topologically stable nodal points, while 3D systems host nodal lines [11–17].

So far, we have restricted the discussion to Hermitian systems. However, in recent years, many studies of NH Hamiltonians have been conducted [23]. The mathematical description of systems with such an effective description is very similar, and in its most general form, a non-interacting, NH two-band system is given by

$$H = d_0\sigma^0 + \mathbf{d}\cdot\boldsymbol{\sigma}, \tag{7}$$

where now d_μ denote *complex valued* continuously differentiable functions of the lattice momentum $\mathbf{k}$. Decomposing $\mathbf{d} = \mathbf{d}_\mathrm{R} + i\mathbf{d}_\mathrm{I}$, the corresponding complex eigenvalues are

$$E_\pm = d_0 \pm \sqrt{d_\mathrm{R}^2 - d_\mathrm{I}^2 + 2i\mathbf{d}_\mathrm{R}\cdot\mathbf{d}_\mathrm{I}}. \tag{8}$$

Hence, the nodal structure is given by the following system of equations,

$$d_\mathrm{R}^2 - d_\mathrm{I}^2 = 0, \quad \mathbf{d}_\mathrm{R}\cdot\mathbf{d}_\mathrm{I} = 0. \tag{9}$$

At this point we set $d_0 = 0$, since we study the topology of the nodal structure, which is not affected by d_0. In contrast to the eigenvalue degeneracies in Hermitian systems, the nodal points in NH systems are *exceptional* (except for when $|\mathbf{d}| = 0$), meaning that not only the eigenvalues, but also the eigenstates coalesce [24]. Also, the exceptional nodal structure is determined by the simultaneous solution of two equations, meaning that stable EPs occur already in 2D systems, while in 3D, they attain the form of closed lines [23]. Notably, as in the case of Hermitian systems, symmetries can be imposed to increase the dimension of the nodal structure. Let us again consider the case of $\mathcal{PT}$ symmetry. Fulfilling Eq. (6) constrains $\mathbf{d}$ as $d_x, d_y \in \mathbb{R}$, $d_z \in i\mathbb{R}$. Clearly, this results in that $\mathbf{d}_\mathrm{R}\cdot\mathbf{d}_\mathrm{I} = 0$ for all $\mathbf{k}$, and the EPs are determined by the solution of only one equation ($d_\mathrm{R}^2 - d_\mathrm{I}^2 = 0$). Hence, stable EPs occur already in symmetric 1D systems, exceptional lines in 2D and exceptional surfaces in 3D [33].

B. Cones of Exceptional Points in $\mathcal{PT}$-symmetric Systems

Let us now focus on the topology of the nodal structure of linear, NH $\mathcal{PT}$-symmetric systems in 3D. A completely general such model with $d_0 = 0$ and with the appropriate choice of coordinates can be put in the form

$$H = (a_x k_x + a_y k_y + a_z k_z + a_0)\,\sigma^x + (b_x k_x + b_y k_y + b_z k_z + b_0)\,\sigma^y + i\,(c_x k_x + c_y k_y + c_z k_z + c_0)\,\sigma^z, \tag{10}$$

with all parameters being real. Explicitly, the corresponding EPs are given by

$$\begin{aligned} &a_0^2 + b_0^2 - c_0^2 + \left(a_x^2 + b_x^2 - c_x^2\right) k_x^2 + \left(a_y^2 + b_y^2 - c_y^2\right) k_y^2 - c_z^2 k_z^2 + 2k_x k_y\,(a_x a_y + b_x b_y - c_x c_y) \\ &- 2c_y c_z k_y k_z - 2c_x c_z k_x k_z + 2k_x\,(a_0 a_x + b_0 b_x - c_0 c_x) - 2k_z c_0 c_z + 2k_y\,(a_0 a_y + b_0 b_y - c_0 c_y) = 0. \end{aligned} \tag{11}$$

Not surprisingly, we can only say that the exceptional nodal structure defines a quadratic surface in momentum space. However, the specific geometry of the exceptional surface can be determined for any choice of parameters. To this end, we consider a linear 2D *Hermitian* $\mathcal{PT}$-symmetric two-band model

$$H = (\eta_x k_x + \eta_y k_y + \eta_0)\,\sigma^0 + (A_x k_x + A_y k_y + A_0)\,\sigma^x + (B_x k_x + B_y k_y + B_0)\,\sigma^y, \tag{12}$$

where all the parameters are real as before. The band structure of this Hamiltonian is necessarily a cone. The eigenvalue equation determining the band structure reads

$$A_0^2+B_0^2-\eta_0^2+\left(A_x^2+B_x^2-\eta_x^2\right)k_x^2+\left(A_y^2+B_y^2-\eta_y^2\right)k_y^2-\lambda^2+2k_xk_y\left(A_xA_y+B_xB_y-\eta_x\eta_y\right)$$
$$+2k_x\lambda\eta_x+2k_y\lambda\eta_y+2k_x\left(A_0A_x+B_0B_x-\eta_0\eta_x\right)+2k_y\left(A_0A_y+B_0B_y-\eta_0\eta_y\right)+2\eta_0\lambda=0, \tag{13}$$

where λ denotes the eigenvalues. Remarkably, this equation is of the same form as Eq. (11). By identifying parameters as $\lambda := \pm c_z k_z$, $A_\mu = a_\mu$, $B_\mu = b_\mu$ and $\eta_\mu = \mp c_\mu$, we see that they exactly coincide. Thus, Eq. (11) is a cone in momentum space. Hence, the exceptional surface of a general 3D NH $\mathcal{PT}$-symmetric linear two-band model attains the form of a stable cone protected by $\mathcal{PT}$ symmetry, from now on referred to as the *exceptional cone* (EC) in momentum space. By stability we mean, just as in the Hermitian case, that an arbitrary symmetry preserving perturbation will merely deform the EC, but will not make it disappear. Interestingly, the tilting of the cone, which in Hermitian systems is governed by the term proportional to σ^0, is in NH $\mathcal{PT}$-symmetric systems controlled by the dissipative term proportional to σ_z. Furthermore, since the EC naturally consists of EPs, $\mathcal{PT}$ symmetry is spontaneously broken exactly on the cone.

Lastly, we want to stress that the relation between the NH EC and the Hermitian energy cone is crucial for the construction of the analogy, which will become clear below.

III. CONES IN BAND STRUCTURES AND LIGHT CONES

The cone-like band structure of certain condensed matter systems, e.g., graphene and WSMs, has in recent years triggered speculations about a possible relation to light cones of observers in the vicinity of a black hole [18]. Concrete studies of such relations have been carried out using different techniques [16, 19–22]. Here, we briefly review the method relating the dispersion of a Dirac operator to a field theory in curved spacetime. We refer the interested reader to Refs. 35 and 36 for a more thorough treatment. What is new is that we also extend this relation to include NH systems by relating the ECs arising in $\mathcal{PT}$-symmetric systems to light cones.

A. Energy Cones and Light Cones

For the sake of illustration, let us consider a tilted Weyl Hamiltonian of the form

$$H = \kappa k_x \sigma^0 + \mathbf{k}\cdot\boldsymbol{\sigma}, \tag{14}$$

where $\kappa \in \mathbb{R}$ is the tilting parameter and $\mathbf{k} := (k_x, k_y, k_z)$. The corresponding energy eigenvalues are given by

$$E_\pm = \kappa k_x \pm \sqrt{k_x^2+k_y^2+k_z^2}. \tag{15}$$

As we mentioned in Section II, $E_\pm$ constitute an upper $(+)$ and a lower $(-)$ part of a cone in energy-momentum space, which touch when $E_+ = E_-$. In Fig. 1, this is illustrated for particular choices of κ. At $|\kappa| > 1$, the energy cone tips over, meaning that $E_\pm$ not only touch, but also cross the Fermi level, forming dimensionful Fermi pockets [which in this case will be infinite as a consequence of Eq. (14) being linear in momentum]. This phenomenon is familiar from the study of Schwarzschild black holes, and made more rigorous by expressing a Dirac-like operator, e.g., the Hamiltonian in Eq. (14) in terms of *vielbeins*, which are related to the metric of a curved spacetime [36]. Explicitly, this yields

$$H = e^i{}_a k_i \sigma^a + e^i{}_0 k_i \sigma^0 \tag{16}$$

with $e^\mu{}_\alpha$ the vielbeins, $\mu, \alpha = 0, x, y, z$ and $i, a = x, y, z$. The corresponding inverse curved spacetime metric is then given by

$$g^{\mu\nu} = e^\mu{}_\alpha e^\nu{}_\beta \eta^{\alpha\beta}, \tag{17}$$

where $\eta^{\alpha\beta} = \mathrm{diag}\,(-1,1,1,1)$ is the Minkowski metric, $e^0{}_0 = 1$ [35], and the other $e^\mu{}_\alpha$ are defined by writing Eq. (14) in the form of Eq. (16). The line element arising from Eq. (17) is

$$ds^2 = -\left(1-\kappa^2\right)dt^2 + (d\mathbf{x})^2 + 2\kappa dx\, dt, \tag{18}$$

where $d\mathbf{x} = (dx, dy, dz)$ and $|d\mathbf{x}|^2 = dx^2 + dy^2 + dz^2$. Eq. (18) describes an event horizon at $|\kappa| = 1$, which coincides exactly with the value of κ where the energy cone described by Eq. (15) is tipped over, cf. Fig. 1.

A natural question to ask at this point is whether or not the resulting artificial event horizon is emitting radiation and, if that is the case, if this can be related to something that can be measured in a laboratory setup. Here we want to make clear that we do not claim that a WSM constitutes a full analogue gravity model. Up to this point, we are noting intuitive similarities between concepts, and we are agnostic about if measurements on WSMs could provide new insights into black hole physics. Interestingly enough, this is something that splits the community. On the one hand, there are works claiming that artificial spontaneous Hawking radiation is present in WSMs [16, 20], while other works claim that there is no radiative process [22]. Intuitively NH systems seem better suited to describe these type of phenomena, due to their natural inclusion of, e.g., gain and loss [23]. Motivated by this, we below suggest an extension of the analogy between Weyl cones and light cones to NH systems.

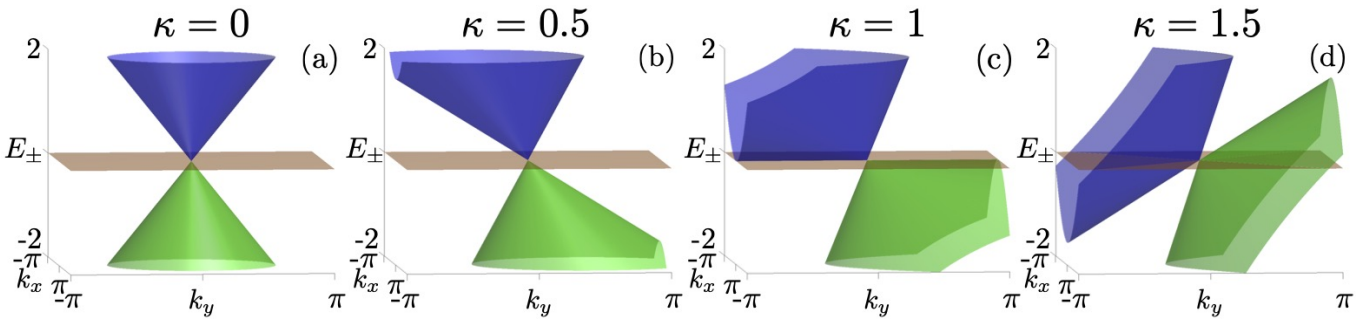

Figure 1. Illustration of the eigenvalues corresponding to Eq. (14) ($k_z = 0$) and Eq. (23) for different values of κ. For $\kappa > 1$, the cone overtilts meaning that the upper and lower band intersect, and not only touch, the Fermi level (brown plane) such that dimensionful Fermi pockets are formed as opposed to the Fermi points that exist when $\kappa < 1$.

B. Exceptional Cones and Light Cones

For the sake of illustration, let us consider the following $\mathcal{PT}$-symmetric two-band toy model

$$H = k_x\sigma^x + k_y\sigma^y + i\left(k_z - \kappa k_x\right)\sigma^z. \tag{19}$$

This system hosts an EC tilted in the k_x-direction with the tilting parameter κ described by

$$k_x^2 + k_y^2 - \left(k_z - \kappa k_x\right)^2 = 0, \tag{20}$$

which is seen by solving for k_z

$$k_z = \kappa k_x \pm \sqrt{k_x^2 + k_y^2}. \tag{21}$$

On the other hand, consider the Hermitian $\mathcal{PT}$-symmetric Hamiltonian

$$H = \kappa k_x\sigma^0 + k_x\sigma^x + k_y\sigma^y \tag{22}$$

with eigenvalues

$$E_\pm = \kappa k_x \pm \sqrt{k_x^2 + k_y^2}. \tag{23}$$

Noting that Eqs. (21) and (23) are similar, the EC attains the exact same form as the energy cone, which can be seen by substituting $E_\pm$ for k_z on the vertical axes in Fig. 1. The quantity k_z can be thought of as the eigenvalue of some Dirac-like operator, e.g.,

$$\hat{k}_z = \kappa k_x\sigma^0 + k_x\sigma^x + k_y\sigma^y. \tag{24}$$

Then, $\hat{k}_z$ can be expressed in terms of vielbeins by using Eq. (16)

$$\hat{k}_z = e^i{}_a k_i\sigma^a + e^i{}_0 k_i\sigma^0, \tag{25}$$

with $i, a = x, y$. This reasoning can be applied straight forwardly to more general $\mathcal{PT}$-symmetric systems, which can be seen by comparing Eqs. (11) and (13), and again thinking of k_z as the eigenvalue of some Dirac-like operator. The artificial light cone is governed by

$$ds^2 = -\left(1 - \kappa^2\right)dt^2 + dx^2 + dy^2 + 2\kappa dx dt, \tag{26}$$

which is obtained by identifying Eqs. (24) and (25), and recalling Eq. (17). This metric has the same form as the one describing the spacetime of a radially infalling observer in the vicinity of a Schwarzschild black hole in Painleveé-Gullstrand coordinates [37]

$$ds^2 = -\left(1 - \frac{2M_0}{r}\right)dT^2 + 2\sqrt{\frac{2M_0}{r}}drdT + dr^2, \tag{27}$$

where M_0 is the mass of the black hole, r the radial coordinate and T the Painlevé time. Considering Eq. (26) in a slice of constant y, and making the identifications $x := r$, $t := T$ and $\kappa := \sqrt{\frac{2M_0}{r}}$, the two metrics indeed coincide.

We need to comment on two caveats before moving on. First, we assume that $dy = 0$, i.e., we consider a slice of constant y. For the analysis in the rest of this work, this amounts to no loss of generality, which will become clear in Section IV. Second, the tilting parameter is promoted to a function with explicit spatial dependence $\kappa = \kappa(r)$, which in principle gives commutator contributions of the form $[H, \kappa(r)] \propto \frac{\partial\kappa(r)}{\partial r}$ to the eigenvalues of the Hamiltonian in Eq. (19). In the following, we ignore those contributions, and provide a rigorous discussion on the consequences of this assumption in Section VI.

So far, we have indeed been able to relate ECs in NH $\mathcal{PT}$-symmetric systems to artificial light cones of observers in the vicinity of a black hole, thus extending the relation previously only valid for Hermitian systems to include NH systems. This was made possible by the relation between NH ECs and Hermitian energy cones, presented in Section II B. The question to ask at this point is: Does the NH system hosting the EC [Eq. (20)] exhibit some dissipative behavior that intuitively can be thought of as artificial Hawking radiation from a stationary Schwarzschild black hole? This question is addressed below.

IV. SPONTANEOUS PARTICLE EMISSION FROM QUANTUM TUNNELING

Classically, black holes only absorb particles. However, when taking quantum mechanical effects close to the horizon

into account, black holes also emit particles, as first shown and interpreted by Hawking [38]. The leading contribution to Hawking radiation comes from light-like (anti) particles tunneling out from (into) the interior of the black hole, as shown by Parikh and Wilczek [39]. The latter is an approximate method accounting only for the leading massless contributions. However, in the semi-classical limit, i.e., when the mass M_0 of the black hole is very large, contributions from massive modes [44] are subleading. For such black holes, the evaporation is slow enough to neglect backreaction effects from the radiation on the metric.

In this section, we apply the techniques developed by Parikh and Wilczek to the NH system given by Eq. (19) to show that there is indeed a non-trivial contribution that can be interpreted as artificial spontaneous Hawking radiation. Consistently, we only consider modes on the EC (in analogy to massless particles propagating along the light cone). To this end, we need to identify the possible particle and antiparticle channels contributing to the total radiation process. Note that the calculations below are carried out in what corresponds to a semi-classical limit, which formally means $M_0 \gg 1$ in the chosen system of units.

A. Legendre Transformation in Non-Hermitian Systems

The quantum tunneling method requires a Lagrangian. For conventional Hermitian systems, the Lagrangian is given by a Legendre transformation of the Hamiltonian

$$L = \mathbf{p} \cdot \dot{\mathbf{q}} - H, \tag{28}$$

where $\mathbf{p}$ denotes the generalized momentum, $\mathbf{q}$ the generalized canonical coordinates and $\dot{f} = \frac{df}{dt}$. This transformation cannot be naively extended to include NH systems. However, using that a general NH Hamiltonian can be decomposed as

$$H = H_1 + iH_2, \tag{29}$$

where, for the specific model considered in Eq. (19), $H_1 = k_x\sigma^x + k_y\sigma^y$ and $H_2 = (k_z - \kappa k_x)\,\sigma^z$ are Hermitian, for each H_i, the conventional Legendre transformation,

$$L_i = \mathbf{k} \cdot \dot{\mathbf{q}} - H_i, \tag{30}$$

holds. Furthermore, the generalized momenta are the same in both H_1 and H_2. Hence, the generalized coordinates and their corresponding time derivative are the same in L_1 and L_2. Thus, the total Lagrangian corresponding to the Hamiltonian in Eq. (19) is given by,

$$L = (1+i)\,\mathbf{k} \cdot \dot{\mathbf{q}} - H. \tag{31}$$

B. Identifying Particle and Antiparticle Channels

When using the quantum tunneling method, the total spontaneous emission is given by the sum of two processes: a particle tunneling out from the interior of the black hole, and an antiparticle tunneling into the interior of the black hole. The quantity of interest, describing classically forbidden trajectories, is the imaginary part of the action of a light-like (anti) particle [39]. Hence, we need to consider the region in momentum space corresponding to the EC [Eq. (20)]. Since the spatial dependence imposed is taken to be in the x-coordinate, we solve Eq. (20) for k_x. Recalling the identification $x := r$, we get

$$k_r^{\pm} = -\frac{\sqrt{2M_0 r}\,k_z}{r-2M_0} \pm \sqrt{\frac{r^2k_z^2}{(r-2M_0)^2} - \frac{rk_y^2}{r-2M_0}}. \tag{32}$$

Since the quantum tunneling takes place close to the horizon $r = 2M_0$, we need not to worry about Eq. (32) taking complex values.

To determine which solution corresponds to (anti) particles, we investigate the behavior of Eq. (32) when $r \to 2M_0$. The dominant term is the singular term in the Laurent expansion of Eq. (32),

$$k_r^{\pm} = \frac{-2M_0k_z \pm r|k_z|}{r-2M_0} + \mathcal{O}\left(r-2M_0\right)^0. \tag{33}$$

Explicitly, we find

$$\lim_{r\to 2M_0^-} k_r^- = \begin{cases} +\infty, & k_z > 0, \\ 0, & k_z \le 0, \end{cases} \tag{34}$$

indicating that k_r^- is the momentum of a *particle* trying to escape from the black hole. Analogously, k_r^+ describes the momentum of an *antiparticle* trying to fall into the black hole,

$$\lim_{r\to 2M_0^+} k_r^+ = \begin{cases} 0, & k_z > 0, \\ +\infty, & k_z \le 0. \end{cases} \tag{35}$$

The singularities indicate that these processes are classically forbidden, and hence quantum tunneling is required to cross the horizon.

C. Quantum Tunneling

We are now ready to calculate the imaginary part of the action for the two-band system. From the Legendre transformation of the Hamiltonian in Eq. (19), the action of the system reads

$$I = \int (1+i)\,k_r dr - \int H dt, \tag{36}$$

which we want to evaluate on the EC. There, the eigenvalues of Eq. (19) coalesce at zero and the last term in Eq. (36) vanishes. Hence, the action on the EC is given by

$$I = \int dr\,(1+i) \times \left[-\frac{\sqrt{2M_0 r}\,k_z}{r-2M_0} \pm \sqrt{\frac{r^2k_z^2}{(r-2M_0)^2} - \frac{rk_y^2}{r-2M_0}}\right], \tag{37}$$

where an implicit sum over the two channels $k_r^{\pm}$ is assumed. From Section IV B, we know that these solutions correspond to the momentum of a particle $(-)$ and antiparticle $(+)$, respectively. For the momentum of a particle, we consider a spontaneous radiation process in which a positive energy ω is assumed to radiate out from the interior of the black hole such that the mass of the black hole changes from M_0 to $M_0-\omega$. The antiparticle case, on the other hand, can be interpreted as a particle propagating backwards in time with a negative energy ω' tunneling inwards such that the mass changes from M_0 to $M_0+\omega'$. We start by considering the contribution from particle tunneling. A particle (with positive energy ω) contributes by tunneling from slightly inside the horizon to outside. Hence the contribution from k_r^- to the action is

$$I_{\mathrm{P}}=\int_{2M_0}^{2(M_0-\omega)}dr\times \left[-\frac{\sqrt{2M_0r}\,k_z}{r-2M_0}-\sqrt{\frac{r^2k_z^2}{(r-2M_0)^2}-\frac{rk_y^2}{r-2M_0}}\right]. \quad (38)$$

Second, to compute the contribution from the antiparticle, we use that the antiparticle is interpreted as a particle with negative energy, ω', that propagates backwards in time. We may thus consider the time-reversed process of a particle with negative energy tunneling into the black hole. A time-reversal transformation sends k_i to $-k_i$, and the contribution to the action from the antiparticle channel is therefore

$$I_{\mathrm{AP}}=\int_{2M_0}^{2\left(M_0+\omega'\right)}dr\times \left[\frac{\sqrt{2M_0r}\,k_z}{r-2M_0}+\sqrt{\frac{r^2k_z^2}{(r-2M_0)^2}-\frac{rk_y^2}{r-2M_0}}\right]. \quad (39)$$

The full action of the system is then given by

$$I=(1+i)\left(I_{\mathrm{P}}+I_{\mathrm{AP}}\right). \quad (40)$$

Now, we expand the integrand around the horizon, $r=2M_0$, and consider the contribution from the singular terms in the Laurent series. After shifting the integration variable, we get,

$$-\int_0^{-2\omega}\frac{4M_0|k_z|}{r'}dr'+\int_0^{2\omega'}\frac{4M_0|k_z|}{r'}dr'. \quad (41)$$

To regularize these integrals we use the Feynman $i\epsilon$ prescription as in Ref. 39. The positive energy ω is sent to $\omega-i\epsilon$, and hence $r'\to r'-i\epsilon$ in the first integral, while the negative energy ω' is sent to $\omega'+i\epsilon$ and $r'\to r'+i\epsilon$ in the second integral. The singular terms then read

$$\begin{aligned}&4M_0|k_z|\lim_{\epsilon\to0}\left(\int_0^{2\omega'}\frac{dr'}{r'+i\epsilon}-\int_0^{-2\omega}\frac{dr'}{r'-i\epsilon}\right)\\&=4M_0|k_z|\lim_{\epsilon\to0}\int_{-2\omega}^{+2\omega}\frac{dr'}{r'-i\epsilon},\end{aligned} \quad (42)$$

where we in the last step used that $\omega=-\omega'$. Remarkably, all the non-singular terms in the Laurent series of I_{P} exactly cancel those in the Laurent series of I_{AP}. As we hinted on in Section III B, the imaginary part of the action is independent of k_y, which justifies setting $dy=0$ in the metric [Eq. (26)], identifying the initial NH band structure to the light cone of a radially infalling observer in the vicinity of an artificial $(3+1)$-dimensional Schwarzschild black hole in Painlevé-Gullstrand coordinates.

Since the only contribution to the action comes from Eq. (42), the action can be evaluated by dividing the contour of integration into two pieces,

$$\begin{aligned}I&=(1+i)\,4M_0|k_z|\lim_{\epsilon\to0}\int_{-2\omega}^{2\omega}\frac{dr'}{r'-i\epsilon}\\&=(1+i)\,4M_0|k_z|\left(\mathrm{P.V.}\int_{-2\omega}^{2\omega}\frac{dr'}{r'}+i\pi\int_{-2\omega}^{2\omega}\delta\left(r'\right)dr'\right)\\&=(1+i)\,4\pi iM_0|k_z|,\end{aligned} \quad (43)$$

giving the imaginary part

$$\mathrm{Im}\left(I\right)=4\pi M_0|k_z|. \quad (44)$$

This indicates that there is indeed a non-vanishing contribution to the classically forbidden imaginary part of the action, and that quantum mechanical effects, such as tunneling, can take place. The probability of a tunneling event can be estimated by the semi-classical emission rate,

$$\Gamma\sim\exp\left(-4\pi M_0|k_z|\right). \quad (45)$$

Recalling that $M_0\gg1$, Γ decays fast with increasing $|k_z|$, which means that a tunneling process is not likely unless $|k_z|$ is small, which we discuss in the following section.

V. INTERPRETATION OF PARTICLE EMISSION AS DISSIPATION

In this section we relate the spontaneous particle emission to the appearance of bulk Fermi states (BFSs) in the initial Hamiltonian (19). This means that we are able to explicitly quantify the dissipation of the NH Hamiltonian in terms of artificial Hawking radiation. Naturally, such a quantification is not possible for Hermitian band structures.

A. Bulk Fermi States and Dissipation

Dissipation in NH Hamiltonians is indicated by topologically protected bulk states, namely BFSs [23]. In general, these are defined by the momentum satisfying

$$\mathrm{Re}\left(E\right)=0\Rightarrow\mathrm{Im}\left(E^2\right)=0,\quad \mathrm{Re}\left(E^2\right)\leq0. \quad (46)$$

Using the Hamiltonian Eq. (19), such dissipative states correspond to

$$k_x^2+k_y^2-\left(k_z-\kappa k_x\right)^2\leq0. \quad (47)$$

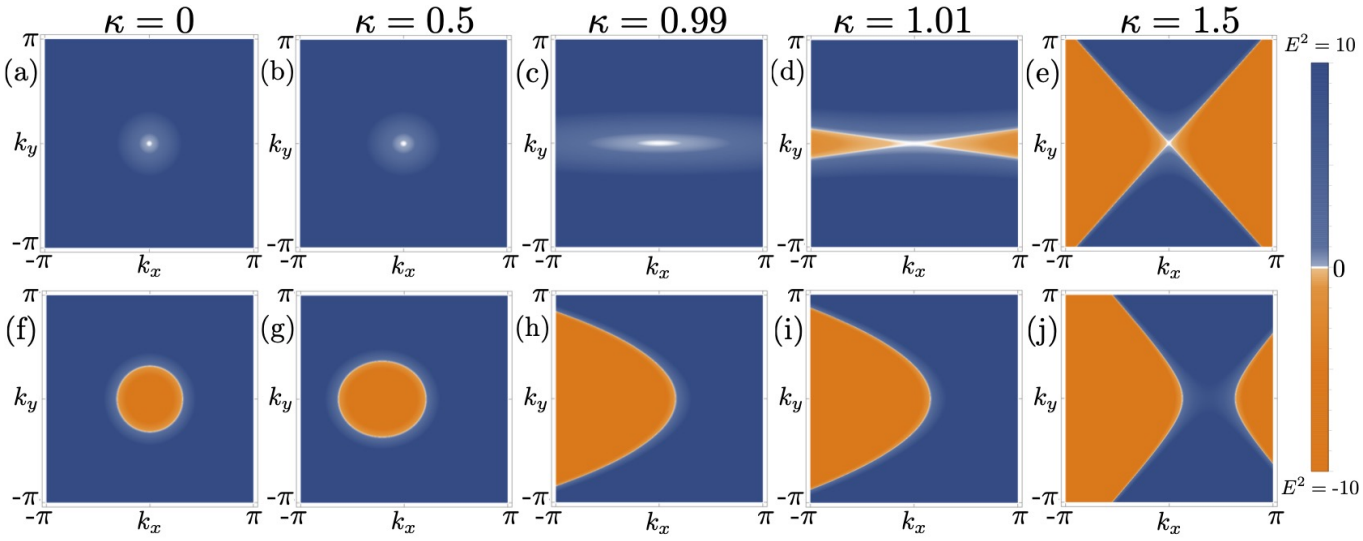

Figure 2. (a)-(e) Bulk Fermi states of the model given by Eq. (19) at $k_z = 0$ for different values of κ. For $\kappa < 1$, the bulk Fermi states are point-like, but as soon as the EC is overtilted, $\kappa > 1$, they form 2D surfaces. This indicates that at $k_z = 0$, there is no dissipative behavior unless $\kappa > 1$. This is due to the formation of a particle-antiparticle pair close to the critical point ($\kappa = 1$). To contrast this, bulk Fermi states of the same model, but at $k_z = \frac{\pi}{2}$, are displayed in (f)-(j), for the same values of κ. For finite k_z, bulk Fermi states are present for all κ, which makes the transition between the regions less clear.

Let us consider Eq. (47) for constant slices of k_z. In Figs. 2 (a)-(e), the BFSs at $k_z = 0$ are displayed for different values of κ. Notably, the BFSs appear when $\kappa > 1$, indicating that dissipative features are present when the EC overtilts. Recalling the expression for the semi-classical emission rate, Eq. (45), we note that we can regard the dissipation at $k_z = 0$ as spontaneous tunneling of light-like particles, which is the leading order contribution to Hawking radiation. We further note that the Hamiltonian Eq. (19) is dissipative also for finite k_z, which is indicated by the existence of BFSs for any value of κ when k_z is non-zero, cf. Figs. 2 (f)-(j). This region is not covered by the quantification in terms of spontaneous emission of light-like particles, cf. Eq. (45) for $M_0 \gg 1$. An interpretation in terms of black-hole physics in this region of momentum space is beyond the scope of this project and hence left as an open question.

B. Artificial Hawking Radiation in Tight-Binding Models

A potential obstacle of the reasoning applied in Section V A is that the BFSs appearing when $\kappa > 1$ for $k_z = 0$ immediately become infinite. This is a direct consequence of Eq. (19) being linear in the momentum components. One way to resolve this is to consider a tight-binding model whose linearized version corresponds to Eq. (19), e.g.,

$$H_{\text{TB}} = \sin k_x \sigma^x + \sin k_y \sigma^y + i\left(\sin k_z - \kappa \sin k_x\right)\sigma^z. \quad (48)$$

Interestingly, the BFSs of this particular model, at $k_z = 0$, are also absent when $\kappa < 1$, cf. Figs. 3 (a)-(c), and they appear as soon $\kappa > 1$, cf. Figs. 3 (d)-(e). This means that the dissipation of the Hamiltonian Eq. (48) at $k_z = 0$ is also explicitly quantified as artificial Hawking radiation, by the reasoning in Section IV. At $k_z = \frac{\pi}{2}$, the BFSs appear rather different than in the linearized model, in particular away from $(k_x, k_y) = (0, 0)$, which is indeed expected, see Figs. 3 (f)-(j). Thus, just as in the linearized model, the dissipation at finite k_z is not quantified as tunneling of light-like particles. Furthermore, for finite k_z there is no clear transition when the EC is overtilted, which can be seen by comparing Figs. 3 (h) and (i), indicating that the interesting change of behavior occurs at $k_z = 0$.

The fact that the tight-binding model in Eq. (48) requires only nearest-neighbor hopping opens the door to possible realizations of systems with ECs in various experimental setups. Potential candidates include disordered and non-equilibrium systems, but also photonic lattices [40, 41], which have recently been used to realize dissipative systems of more complicated nature [42]. Since Hawking radiation in stationary Schwarzschild black holes appears as quantum fluctuations of an otherwise classical system, it would be intriguing to investigate photonic crystals and see if similar phenomena related to spontaneous emission of particles can be observed. Suggestive methods include ARPES measurements to image the BFSs at $k_z = 0$ and around $\kappa = 1$. Tuning κ to vary slowly with respect to space around $\kappa = 1$, the transition illustrated in Figs. 3 (c) and (d) should be observable.

VI. DISCUSSION AND OUTLOOK

One of the first assumptions we made when modelling the artificial Schwarzschild event horizon, was to neglect the commutator contributions occurring when the tilting parameter κ was assigned an explicit spatial dependence. Let us now investigate what this means. The neglected commutators turn

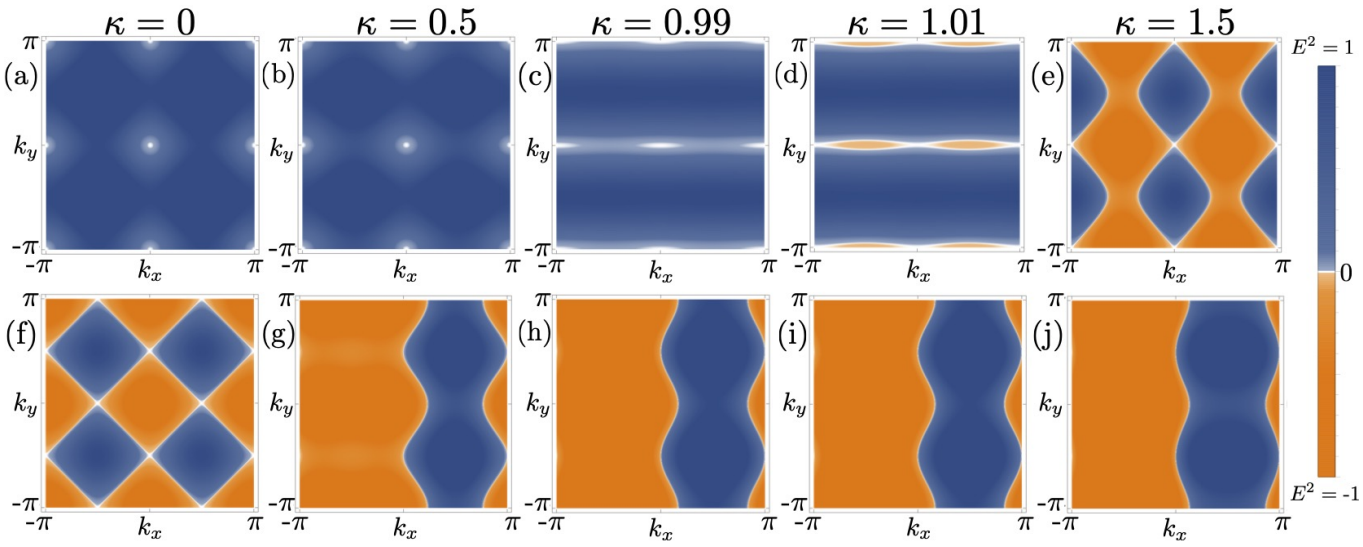

Figure 3. (a)-(e) Bulk Fermi states of the model given by Eq. (48) at $k_z = 0$ for different values of κ. As in Fig. 2, the bulk Fermi states are point-like when $\kappa < 1$, but attain the form of 2D surfaces when the EC is overtilted. In the regime where the linear approximation is motivated, this can be interpreted as a spontaneous creation and emission of a particle-antiparticle pair around $\kappa = 1$. For finite k_z, illustrated for $k_z = \frac{\pi}{2}$ in (f)-(j), there is no clear difference between the cases when $\kappa < 1$ and $\kappa > 1$, which indicates $k_z = 0$ is indeed the point of interest.

out to be proportional to a more simple commutator. This can be seen by explicitly plugging in the expression for the Hamiltonian from Eq. (19) and recalling the identification $x := r$. This yields

$$[H, \kappa(r)] \propto [k_r, \kappa(r)]\,, \tag{49}$$

and

$$[H, k_r] \propto [k_r, \kappa(r)]\,, \tag{50}$$

and evaluates to

$$[k_r, \kappa(r)] \propto \frac{\partial \kappa(r)}{\partial r} \propto \frac{M_0}{r^2\sqrt{\frac{2M_0}{r}}}. \tag{51}$$

When moving away from the horizon this goes as $r^{-3/2}$, and thus decays for increasing r. However, the quantum tunneling occurs close to the horizon, and therefore, we also have to make sure that it is well motivated to neglect the commutator there. At the horizon, the commutator is

$$[k_r, \kappa(r)]|_{r=2M_0} \propto M_0^{-1}. \tag{52}$$

As we assumed $M_0 \gg 1$, this contribution indeed disappears.

We note that the current study exclusively deals with stationary phenomena, both in terms of black holes and in terms of topological phases. Previous works in the Hermitian realm have used a Lagrangian formalism to study the time-dependence of solutions to the Euler-Lagrange equations [22]. These are shown to not result in any radiative behavior over time, indicating that Hermitian systems model artificial black holes in equilibrium. Unfortunately, similar studies cannot be extended in a straightforward manner to NH systems, since the conventional stationary action principle is not applicable. The action corresponding to a NH Hamiltonian necessarily becomes complex, and hence one would have to choose whether to minimize, e.g., its real part, imaginary part or absolute value. Instead, we suggest that time dependence can be introduced differently into NH Hamiltonians through dissipation. Including time as an explicit variable in the Hamiltonian requires a more thorough relation to the gravitational side [21, 36]. In principle, in such an analogy, the time-dependent dissipation could be used to mimic black hole evaporation. The latter remains an open question in the current setup.

We also note that the creation (and emission) of the particle-antiparticle pair occurs exactly on the EC, where $\mathcal{PT}$ symmetry is spontaneously broken. This has, to our knowledge, not been observed before and should be investigated in other setups to see whether or not it is a generic feature. However, this is beyond the scope of this article.

In recent works, the importance of additional bands in similar NH models has been studied [45, 46]. In particular, the appearance of higher order EPs is investigated. To this point, we note that considering additional bands, the ECs of order two can be accompanied by third order exceptional lines and fourth order EPs in 3D $\mathcal{PT}$-symmetric systems. The impact of the higher order exceptional structure is something that we find interesting, but nothing that we intend to investigate at this point. Here we assume the additional bands to be located far away from the ones considered in this work, and leave further investigation for future studies.

VII. CONCLUSION

In this work, we have studied the topology of the exceptional nodal structures in linear 3D NH two-band models sub-

ject to $\mathcal{PT}$ symmetry. We showed that the EPs constitute a symmetry-protected EC in momentum space by relating the EC to the energy cone of a 2D Hermitian $\mathcal{PT}$-symmetric Hamiltonian. By using what was already known for Hermitian systems, we were able to find a relation between the EC and the light cone of a radially infalling observer in the vicinity of a stationary Schwarzschild black hole. Notably, the exact same light cone was obtained from the Hermitian Hamiltonian. By applying the quantum tunneling method [39] to the NH system, we explicitly showed that a light-like particle-antiparticle pair was created on and emitted from the EC, where $\mathcal{PT}$ symmetry is spontaneously broken, at the point of critical tilting. We then interpreted this spontaneous emission in terms of the existence of BFSs.

We thus extended the previously known Hermitian relation to artificial light cones to include NH systems. This allowed for the interpretation of spontaneous Hawking radiation as dissipative features, which was not possible for Hermitian systems. Interestingly, recent studies show that NH systems can be related to general features of quantum gravity [47, 48], indicating further interpretations and applications of non-Hermiticity in the study of the nature of spacetime. Hopefully, further studies will sharpen and clarify the analogy between dissipative NH systems and black hole physics.

ACKNOWLEDGEMENTS

We would like to thank Emil J. Bergholtz, Johan Carlström and Watse Sybesma for useful discussions. Special thanks to Thors Hans Hansson, Igor Pikovski, Bo Sundborg and Lárus Thorlacius for useful comments on the manuscript. M.S. is supported by the Swedish Research Council (VR) and the Wallenberg Academy Fellows program of the Knut and Alice Wallenberg Foundation. L.R. is supported by the Knut and Alice Wallenberg foundation under grant no. 2017.0157. F.K.K. is supported by the Max Planck Institute of Quantum Optics (MPQ) and Max-Planck-Harvard Research Center for Quantum Optics (MPHQ).

[1] K.v. Klitzing, G. Dorda, and M. Pepper, *New Method for High-Accuracy Determination of the Fine-Structure Constant Based on Quantized Hall Resistance*, Phys. Rev. Lett. **45**, 494 (1980), doi:10.1103/PhysRevLett.45.494.

[2] M.Z. Hasan and C.L. Kane, *Colloquium: Topological insulators*, Rev. Mod. Phys. **82**, 3045 (2010), doi: 10.1103/RevModPhys.82.3045.

[3] X.-L. Qi and S.-C. Zhang, *Topological insulators and superconductors*, Rev. Mod. Phys. **83**, 1057 (2011), doi: 10.1103/RevModPhys.83.1057.

[4] M.O. Goerbig, *Electronic properties of graphene in strong magnetic field*, Rev. Mod. Phys. **83**, 1193 (2011), doi: 10.1103/RevModPhys.83.1193.

[5] N.P. Armitage, E.J. Mele, and A. Vishwanath, *Weyl and Dirac semimetals in three-dimensional solids*, Rev. Mod. Phys. **90**, 015001 (2018), doi:10.1103/RevModPhys.90.015001.

[6] J.C. Budich and B. Trauzettel, *From the adiabatic theorem of quantum mechanics to topological states of matter*, physica status solidi (RRL) **7**, 109 (2013), doi:10.1002/pssr.201206416.

[7] H. Weyl, *Elektron und Gravitation. I*, Z. Physik **56**, 330 (1929), doi:10.1007/BF01339504.

[8] S.-Y. Xu, I. Belopolski, N. Alidoust, M. Neupane, G. Bian, C. Zhang, R. Sankar, G. Chang, Z. Yuan, C.-C. Lee, S.-M. Huang, H. Zheng, J. Ma, D.S. Sanchez, B. Wang, A. Bansil, F. Chou, P.P. Shibayev, H. Lin, S. Jia, and M.Z. Hasan, *Discovery of a Weyl fermion semimetal and topological Fermi arcs*, Science **349**, 613 (2015), doi:10.1126/science.aaa9297.

[9] B.Q. Lv, H.M. Weng, B.B. Fu, X.P. Wang, H. Miao, J. Ma, P. Richard, X.C. Huang, L.X. Zhao, G.F. Chen, Z. Fang, X. Dai, T. Qian, and H. Ding, *Experimental Discovery of Weyl Semimetal TaAs*, Phys. Rev. X **5**, 031013 (2015), doi: 10.1103/PhysRevX.5.031013.

[10] L. Lu, Z Wang, D. Ye, L. Ran, L. Fu, J. D. Joannopoulos, and M. Soljacic, *Experimental observation of Weyl points*, Science **349**, 6248, 622-624 (2015), doi:10.1126/science.aaa9273.

[11] C. Herring, *Accidental Degeneracy in the Energy Bands of Crystals*, Phys. Rev. **52** 365 (1937), doi: 10.1103/PhysRev.52.365.

[12] M. Ezawa, *Topological semimetals carrying arbitrary Hopf numbers: Fermi surface topologies of a Hopf link, Solomon's knot, trefoil knot, and other linked nodal varieties*, Phys. Rev. B **96**, 041202(R) (2017), doi:10.1103/PhysRevB.96.041202.

[13] Z. Yan, R. Bi, H. Shen, L. Lu, S.-C. Zhang, and Z. Wang, *Nodal-link semimetals*, Phys. Rev. B **96**, 041103(R) (2017), doi:10.1103/PhysRevB.96.041103.

[14] G. Chang, S.-Y. Xu, X. Zhou, S.-M. Huang, B. Singh, B. Wang, I. Belopolski, J. Yin, S. Zhang, A. Bansil, H. Lin, and M.Z. Hasan, *Topological Hopf and Chain Link Semimetal States and Their Application to Co_2MnGa*, Phys. Rev. Lett. **119**, 156401, doi:10.1103/PhysRevLett.119.156401.

[15] L. Li, C.H. Lee, and J. Gong, *Realistic Floquet Semimetal with Exotic Topological Linkages between Arbitrarily Many Nodal Loops*, Phys. Rev. Lett. **121**, 036401, doi: 10.1103/PhysRevLett.121.036401.

[16] G.E. Volovik, and K. Zhang, *Lifshitz Transitions, Type-II Dirac and Weyl Fermions, Event Horizon and All That*, J. Low Temp. Phys. **189**, (2017), doi:10.1007/s10909-017-1817-8.

[17] R. Bi, Z. Yan, L. Lu and Z. Wang, *Nodal-knot semimetals*, Phys. Rev. B **96**, 201305 (2017), doi:10.1103/PhysRevB.96.201305.

[18] C. Beenakker, Commentary at the Journal Club for Condensed Matter Physics (2015), https://www.condmatjclub.org/?p=2644.

[19] M.A. Zubkov, *Analogies between the Black Hole Interior and the Type II Weyl Semimetals*, Universe 2018, **4 (12), 135**, doi:10.3390/universe4120135.

[20] H. Liu, J.-T. Sun, H. Huang, F. Liu, and S. Meng, *Fermionic analogue of black hole radiation with a super high Hawking temperature*, arXiv:1809.00479.

[21] G.E. Volovik, and M.A. Zubkov *Emergent Weyl spinors in multi-fermion systems*, Nuclear Physics, B **881** (2014), doi: 10.1016/j.nuclphysb.2014.02.018.

[22] Y. Kedem, E.J. Bergholtz, and F. Wilczek *Black and White Holes at Matetrial Junctions*, Phys. Rev. Research **2**, 043285 (2020), doi:10.1103/PhysRevResearch.2.043285.

[23] E.J. Bergholtz, J.C. Budich, and F.K. Kunst, *Exceptional topology of non-Hermitian systems*, Rev. Mod. Phys **93**, 015995 (2021), doi:10.1103/RevModPhys.93.015005.

[24] D.C. Brody, *Biorthogonal quantum mechanics*, Journal of Physics A: Math. Theor. **47** 034305 (2014), doi:10.1088/1751-8113/47/3/035305.

[25] M. Berry, *Physics of Nonhermitian Degeneracies*, Czechoslovak Journal of Physics **54**, 1039 (2004), doi: 10.1023/B:CJOP.0000044002.05657.04.

[26] J. Carlström and E.J. Bergholtz, *Exceptional links and twisted Fermi ribbons in non-Hermitian systems*, Phys. Rev. A **98**, 042114 (2018), doi:10.1103/PhysRevA.98.042114.

[27] R.A. Molina and J. Gonzalez, *Surface and 3D Quantum Hall Effects from Engineering of Exceptional Points in Nodal-Line Semimetals*, Phys. Rev. Lett. **120**, 146601 (2018), doi:10.1103/PhysRevLett.120.146601.

[28] K. Moors, A.A. Zyuzin, A.Y. Zyuzin, R.P. Tiwari and T.L. Schmidt, *Disorder-driven exceptional lines and Fermi ribbons in tilted nodal-line semimetals*, Phys. Rev. B **99**, 041116(R) (2019), doi:10.1103/PhysRevB.99.041116.

[29] V. Kozii and L. Fu, *Non-Hermitian Topological Theory of Finite-Lifetime Quasiparticles: Prediction of Bulk Fermi Arc Due to Exceptional Point*, arXiv:1708.05841 (2017).

[30] J. Carlström, M. Stålhammar, J.C. Budich, and E.J. Bergholtz, *Knotted Non-Hermitian Metals*, Phys. Rev. B **99**, 161115(R) (2019), doi:10.1103/PhysRevB.99.161115.

[31] C.H. Lee, G. Li, Y. Liu, T. Tai, R. Thomale, and X. Zhuang, *Tidal surface states as fingerprints of non-Hermitian nodal knot metals*, Communications Physics **4**, 47 (2021), doi: 10.1038/s42005-021-00535-1.

[32] M. Stålhammar, L. Rødland, G. Arone, J.C. Budich and E.J. Bergholtz, *Hyperbolic nodal band structures and knot invariants*, SciPost Physics **7**, 019 (2019), doi: 10.21468/SciPostPhys.7.2.019.

[33] J.C. Budich, J. Carlström, F.K. Kunst, and E.J. Bergholtz, *Symmetry-protected nodal phases in non-Hermitian systems*, Phys. Rev. B **99**, 041406(R), doi: 10.1103/PhysRevB.99.041406.

[34] C.M. Bender, and S. Boettcher, *Real Spectra in Non-Hermitian Hamiltonians Having $\mathcal{PT}$ Symmetry*, Phys. Rev. Lett. **80**, 4243 (1998), doi:10.1103/PhysRevLett.80.5243.

[35] G.E. Volovik, *The Universe in a Helium Droplet* (Clarendon, Oxford, 2003), doi: 10.1093/acprof:oso/9780199564842.001.0001.

[36] P. Hořava, *Stability of Fermi Surfaces and K-Theory*, Phys. Rev. Lett. **95**, 016405 (2005), doi:10.1103/PhysRevLett.95.016405.

[37] P. Painlevé, *La mécanique classique et la théorie de la relativité*, C. R. Acad. Sci. (Paris) **173**, (1921).

[38] S.W. Hawking, *Particle creation by black holes*, Comm. Math. Phys. **43**, 199 (1975), doi:10.1007/BF02345020.

[39] M.K. Parikh and F. Wilczek, *Hawking Radiation as Tunneling*, Phys. Rev. Lett. **85**, 5042 (2000), doi: 10.1103/PhysRevLett.85.5042.

[40] L Lu, J.D. Joannopoulos, and M. Soljačič, *Topological Photonics*, Nature Photonics **8** (2014), doi:10.1038/nphoton.2014.248.

[41] B.A. Bell, K. Wang, A.S. Solntsev, D.N. Neshev, A.A. Sukhorukov, and B.J. Eggleton, *Spectral photonic lattices with complex long-range coupling*, Optica **4**, 11 (2017), doi:10.1364/OPTICA.4.001433.

[42] K. Wang, L. Xiao, J.C. Budich, W.Yi, and P. Xue, em Simulating Exceptional Non-Hermitian Metals with Single-Photon Interferometry, arXiv:2011.01884.

[43] H. Zhou, C. Peng, Y. Yoon, C. W. Hsu, K. A. Nelson, L. Fu, J. D. Joannopoulos, M. Soljačič, and B. Zhen, *Observation of bulk Fermi arc and polarization half charge from paired exceptional points*, Science **359**, 6379 (2018), doi: 10.1126/science.aap9859.

[44] A. Coutant, A. Fabbri, R. Parentani, R. Balbinot, and P.R. Anderson, *Hawking radiation of massive modes and undulations*, Phys. Rev. D **86** 064022 (2012), doi: 10.1103/PhysRevD.86.064022.

[45] I. Mandal, and E.J. Bergholtz, *Symmetry and Higher-Order Exceptional Points*, arXiv:2103.15729.

[46] P. Delplace, T. Yoshida, and Y. Hatsugai, *Symmetry-protected higher-order exceptional points and their topological characterization*, arXiv:2103.08232.

[47] C. Lv, R. Zhang and Q. Zhou, *Curving the space by non-Hermiticity*, arXiv:2106.02477.

[48] L. M. Lawson, *Minimal and maximal lengths from position-dependent non-commutativity*, arXiv:2012.06906.